Scientific Research Publishing

Open Journal of Geology, 2024, 14, 594-616
https://www.scirp.org/journal/ojg
ISSN Online: 2161-7589
ISSN Print: 2161-7570

Gravity-Driven Listric Growth Fault and Sedimentation in the Lagoa do Peixe, Rio Grande do Sul Coastal Plain, Brazil

Bruno Silva da Fontoura[1], Adelir José Strieder[2*], Iran Carlos Stalliviere Corrêa[1], Paulo Rogério Mendes[3]

[1]Instituto de Geociências, UFRGS, Porto Alegre, Brazil
[2]Engenharia Geológica, Centro de Engenharias, UFPel, Pelotas, Brasil
[3]HIDROSERV—Serviços Geológicos e Geofísicos Ltda., Porto Alegre, Brazil
Email: *adelirstrieder@outlook.com

How to cite this paper: da Fontoura, B.S., Strieder, A.J., Corrêa, I.C.S. and Mendes, P.R. (2024) Gravity-Driven Listric Growth Fault and Sedimentation in the Lagoa do Peixe, Rio Grande do Sul Coastal Plain, Brazil. *Open Journal of Geology*, **14**, 594-616.
https://doi.org/10.4236/ojg.2024.144025

Received: March 11, 2024
Accepted: April 23, 2024
Published: April 26, 2024

Abstract

High frequency, high resolution GPR surveys are successfully applied to investigate near-surface stratification architecture of sedimentary units in coastal plains and to define their depositional conditions. However, low frequency GPR surveys to investigate fault-related depositional systems at greater depths are scarce. This survey was designed investigate a > 100 km long linear escarpment that controls the northwest margin of the Lagoa do Peixe, an important lagoon in Rio Grande do Sul Coastal Plain (RGSCP, Brazil). The traditional approach points that RGSCP was developed by juxtaposition of four lagoons/barrier systems as consequence of sea level changes; no deformational structure is admitted to exist before. The low frequency GPR (50 MHz, RTA antenna) and geological surveys carried out in the RGSCP showed the existence of a large, gravity-driven listric growth fault controlling the Lagoa do Peixe escarpment and hangingwall sedimentation. The radargrams in four subareas along the Lagoa do Peixe Growth Fault could be interpreted following the seismic expression of rift-related depositional systems. The radargrams enabled to distinguish three main lagoonal deposition radarfacies. The lower lagoonal radarfacies is a convex upward unit, thicker close to growth fault; the radarfacies geometry indicates that fault displacement rate surpasses the sedimentation rate, and its upper stratum is aged ~3500 ^{14}C years BP. The second lagoonal radarfacies is a triangular wedge restricted to the lagoon depocenter, whose geometry indicates that fault displacement and the sedimentation rates kept pace. The upper lagoonal radarfacies is being deposited since 1060 ± 70 ^{14}C years BP, under sedimentation rate higher than fault displacement rate. The results indicate that low frequency GPR surveys can help in

investigating fault-related depositional systems in coastal zones. They also point to a new approach in dealing with RGSCP stratigraphy.

Keywords

GPR (Ground-Penetrating Radar), Growth Fault, Sedimentation, Radarfacies, Coastal Plain

1. Introduction

The Rio Grande do Sul Coastal Plain (RGSCP) is the emerged part of the gently sloping Pelotas Basin continental shelf, the southernmost of Brazil's Atlantic basins. This coastal plain is up to 100 km wide and extends for more than 600 km. The RGSCP was formed by juxtaposition of sedimentary deposits derived from deltaic alluvial plains and four lagoons/barrier systems developed as consequence of sea level changes from Middle Pleistocene to Holocene [1]. The first lagoon/barrier system (I) has an estimated age of 325 ka. The following systems have absolute ages of 230 ka (II), 123 - 125 ka (III), and 5.6 ka (IV) MIS according to [2] (**Figure 1**).

The RGSCP lagoons/barrier system was defined based on sedimentary facies, depositional systems, and chronostratigraphic techniques [3] and [4]. No neotectonic deformational episode is considered for RGSCP lagoons/barrier sedimentary strata juxtaposition: "*the Pelotas Basin has remained oblivious to major tectonic movements, which translates into the symptomatic absence of faulting. If there were any, they resulted from aseismic processes in the sedimentary package that today constitutes the slope of the continental margin*" [5].

Recently, some records of neotectonic activity in the RGSCP have been identified. Fonseca [6] produced a wide investigation for neotectonic records in the RGSPC based on geomorphic features, small-scale field structures, and remote sensing images (LANDSAT, SRTM). He [6] was also able to identify significant neotectonic records and "*suggested systematic campaigns of field to structural and geophysical data-collecting in the identified areas*". Strieder *et al.* [7] showed preliminary evidence of major faults controlling Lagoa do Peixe and discussed some implications for RGSCP. Cooper *et al.* [8] and [9] have also showed evidence for major deformation in the Santa Catarina Coastal Plain. da Fontoura *et al.* [10] also described and discussed a series of leading normal faults controlling the beach ridges progradation in the Quinta-Cassino area of the RGSCP.

The aim of this paper is to show a large-scale fault in the RGSCP, which cuts across Pleistocene coastal barrier (III) and controls Holocene barrier (IV) and lagoon system development. 50 MHz RTA Ramac GPR surveys, drillholes and field surveys were carried out in order to determine the regional structural framework developed by the Lagoa do Peixe Growth Fault. The paper also discusses the sedimentation processes under the influence of mechanical subsidence.

The paper explores i) the surface, exposed geology to ensure the best location

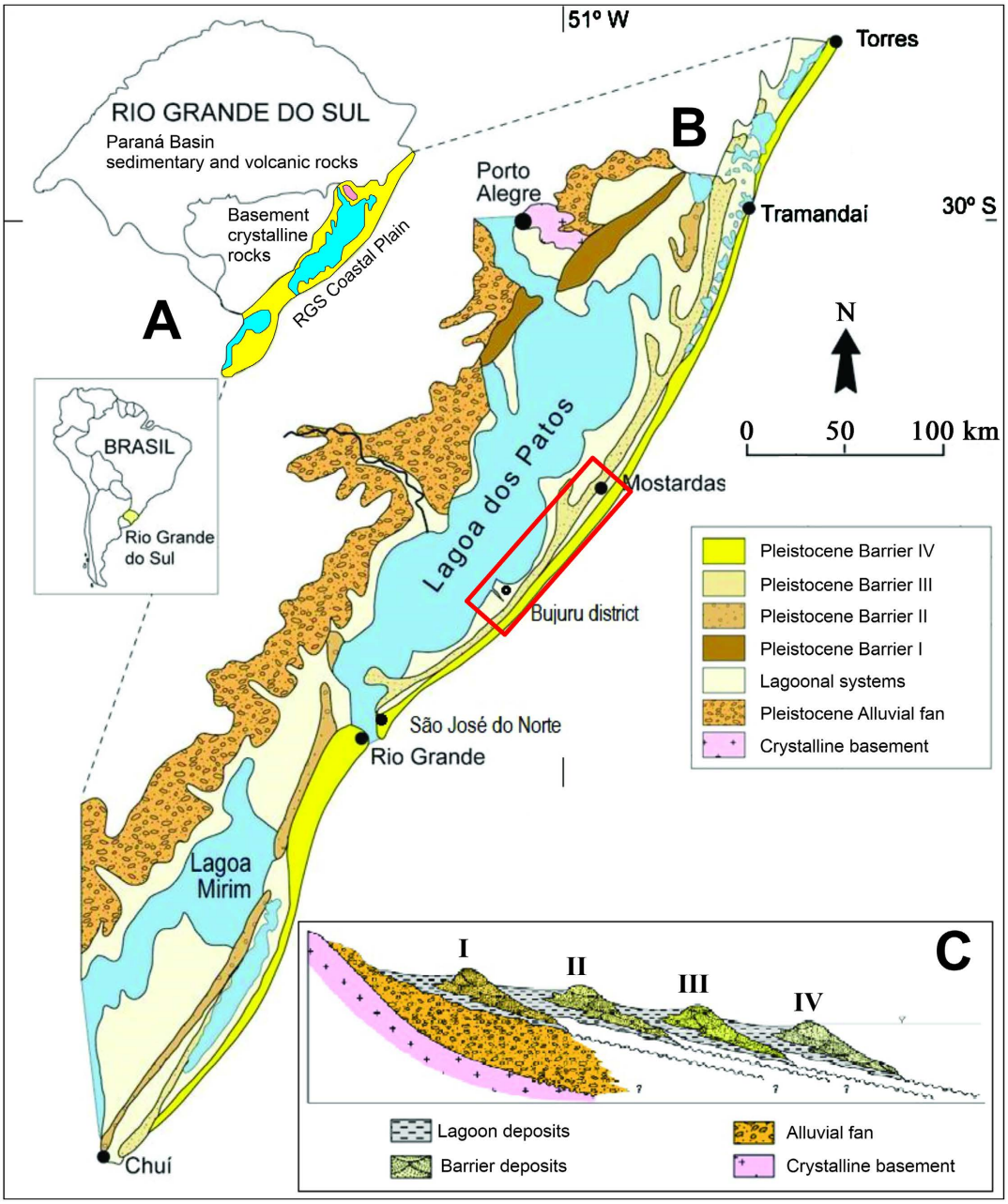

Figure 1. Rio Grande do Sul Coastal Plain location (A), its regional geological map (B), and the model for its depositional systems (C). Modified from [3] and [4], the red rectangle circunscribes the area of investigation in **Figure 2**.

for GPR profiles and drillholes, as also as to understand the Holocene terrain geomorphology, ii) presents the processed and interpreted radargrams showing the most important faults and their relationships with radarfacies, both unexposed and exposed ones. These data, then, are discussed to propose a Holocene geological evolution of the Lagoa do Peixe Growth Fault and sedimentation it controlled. Some published ^{14}C age determinations (peat and shells) evaluated, chiefly those sampled in known radarfacies here investigated, in order to reconstruct the evolving Lagoa do Peixe area under the influence of this growth fault.

2. Geophysical and Geological Survey Methods

The Lagoa do Peixe is a National Park, a conservation unit established due to Decree n˚ 93.546/1986 (Figure 2). The Lagoa do Peixe, in fact a lagoon, is home to large amounts of migratory birds coming from the Northern (summer) and Southern (winter) hemispheres.

The northwestern border of the Lagoa do Peixe is a steep escarpment, whose actual altitude differences amount up to 10 m. This escarpment is close to deeper water sheet, which is poorly maintained during the dry season of the La Niña periods. The southeastern border is gently dipping toward northwest, and its connection with Atlantic Ocean is cancelled during the dry seasons.

The Lagoa do Peixe escarpment was previously regarded as a geomorphic lineament possibly due to a neotectonic structure [6]. This geomorphic lineament is clearly defined in satellite images as a N40E trending, >100 km long escarpment. Based on these geomorphic features, four areas for geophysical and geological survey were selected: i) Mostardas (northern), ii) Tavares (central), iii) Lagoa do Cará, and iv) Bujuru (see Figure 2 for details). The surveyed areas were focused to investigate what kind of geological structure controls the escarpment in

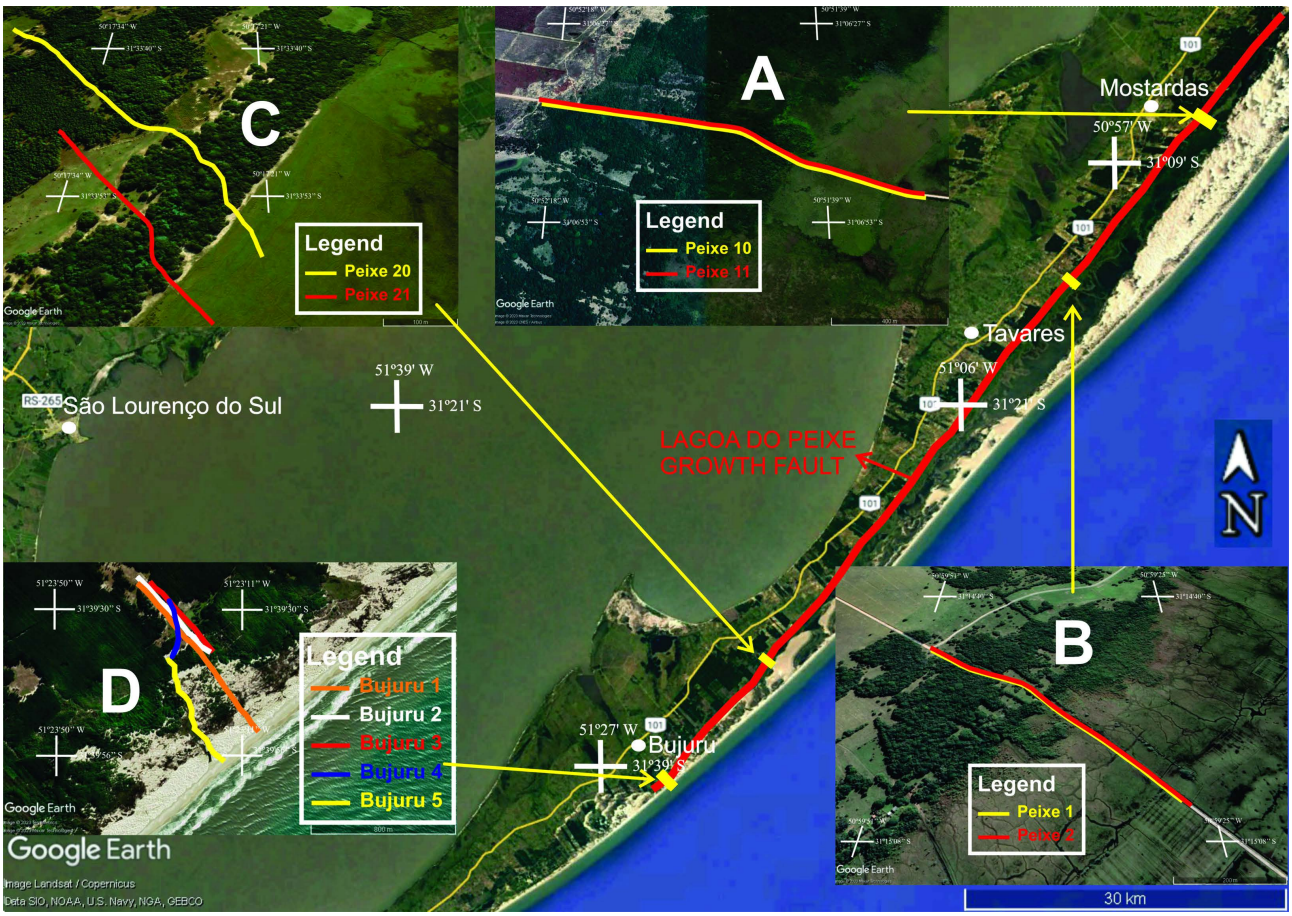

Figure 2. Location of the Lagoa do Peixe Growth Fault and the areas of detailed geological and geophysical surveying. (A) Mostardas (northern), (B) Tavares (central), (C) Lagoa do Cará, and (D) Bujuru (Southern) areas. The length of each GPR line is presented its respective radargram in Figure 7, Figures 9-11.

its entire extend.

The geophysical surveys were carried out through 50 MHz RTA Ramac equipment. This frequency was selected to investigate that structure as deep as possible (>20 m depth was attained with good resolution). The mean EM wave velocity was estimated to be 0.08 m/ns, so that vertical resolution is ~0.8 m. Then, the EM wavelength is not adequate small-scale structures of sedimentary units, but to their geometry and continuity. Low frequence antennas have higher limitations in distinguishing types of sediments, unless they show well contrasting EM properties and make up thicker beds. In this way, a careful GPR survey was conducted, and profile location was selected according to surface geological investigation to maximize GPR signal.

Two parallel GPR lines were surveyed in Mostardas, Tavares and Lagoa do Cará areas. The Mostardas and Tavares GPR lines were surveyed in gravel roads cutting across Lagoa do Peixe. Lagoa do Cará (a lake isolated from the main Lagoa do Peixe due to sedimentation) was profiled in a secondary road as long as possible into the clogged lagoon. In the Bujuru area, five parallel and oblique lines were surveyed, since no water filled depression is present and a better scanning for the fault geometry can be produced.

Post-processing used Reflex-W software and included the following main steps: dewow filter; bandpass filter (butterworth, but sometimes trapezoidal); migration (v = 0.297 m/ns) for removing surface reflections in unshielded antenna; topographic correction; 3D topographic migration (e.g. v = 0.08 m/ns) and butterworth filtering.

The GPR survey lines were all accompanied by DGPS (Emlid, Reach RS+ model, base and rover receptors) control, with kinematic and post-processed corrections (Leica Geo Office and PPP-IBGE). The GPR line positioning procedure does permit a high horizontal (7 mm + 1 ppm), and vertical precisions (14 mm + 1 ppm).

The Bujuru area was drilled to determine the sand thickness covering the peat layer, and the stratigraphic features of the Pleistocene barrier (III). Three percussion drill cores were sampled and correlated with GPR survey line (Bujuru01 line). It was selected to drill because the peat layer does not crop out in the actual beach, and the GPR survey line ends at beach; thus, it was possible to control the geophysical signature of the peat layer.

3. Geology of the Surveyed Areas

The geologic survey of the detailed areas was carried out through aerial-photographs, high resolution Google images, and field work. The aim of the geologic survey was to investigate the main surficial sedimentary units over which GPR survey lines were conducted, to define their main geological features that can contribute to discriminate them in radargrams. The aim was not to fully characterize each sedimentary unit in terms of their sedimentological properties.

Figures 3-6 present simplified geological maps that are result of aerial photo-

graphs, Google high resolution images and field work. Table 1 summarizes the main lithological features of each stratigraphic unit distinguished during the geological survey.

The Pleistocene Barrier III is a key stratigraphic unit for GPR surveys since it rests as a structural high west of the Lagoa do Peixe Growth Fault scarp. This structural high may be recognized in two erosional tiers (10 - 15 m, and 5 - 8 m) above mean see level (see Figure 3(B), Tavares geological map). It is best exposed in the Talhamar Road (Tavares area), at the erosional retreating fault scarp (Figure 4(B)). On the other side, the west limit of the Pleistocene Barrier III is not fault bounded, but erosional, as can be seen by several embayment controlled by actual drainage.

The Holocene Lagoonal deposits rest at <3 m above mean see level. Parallel stratification of silts and fine-grained sands and peat rich layers or lenses (≥0.5 m thick) are present. An upper peat layer crops out in some segments along the beach in the investigated area when it is being eroded. A gentle folding and faulting of this upper peat layer controls its outcropping.

The Holocene Lagoonal deposits are also present in the west limit of the Pleistocene Barrier III structural high, where they are under the influence of the Lagoa dos Patos. These lagoonal deposits are not in the scope of this investigation, since their actual limits are not fault-bounded.

The Holocene Barrier IV system is under construction close to the Atlantic Ocean. It is made up by aeolian dunes migrating from NE toward SW. This dune system discordantly overlays the Holocene Lagoonal deposits in the Lagoa do Peixe National Park. This feature is best recognized in segments where the upper peat layer crops out and is under erosion. In some places, where actual active dunes are not present, is possible to recognize a previous, vegetated dune blanket that seems to have been developed by winds blowing more easterly. The Holocene Barrier IV system advances over and clogs the eastern margin of the Lagoa do Peixe, as can be seen in Figures 3-6.

Table 1. Summary of the main stratigraphic units cropping out in the selected areas for GPR surveying.

Stratigraphic unit		Geological and lithological features
Transgressive Aeolian covers		Thin transgressive dune sheets (TDS) (< 1 m thick) of fine-grained sands covering mainly the structural highs (Barrier III). Locally, it can develop a small transgressive dune up to 2 - 3 m high.
BARRIER IV	Holocene Barrier **B**	Active transgressive dunes close to the Atlantic Ocean, making part of the actual dune system building the Holocene Barrier IV.
	Holocene Barrier **A**	Inactive transgressive dunes underlying the active ones. They seem to be coarser grained than actual ones and are anchored by native grass and bushes.
Holocene Lagoonal deposits		Fine-grained sands and silts interlayered with variable proportions of organic matter and clays in depressed areas.
Pleistocene Barrier III		Fine to medium-grained sands, mostly horizontal, parallel stratification, slightly compacted, and impregnated by Fe^{3+} hydroxides and clay.

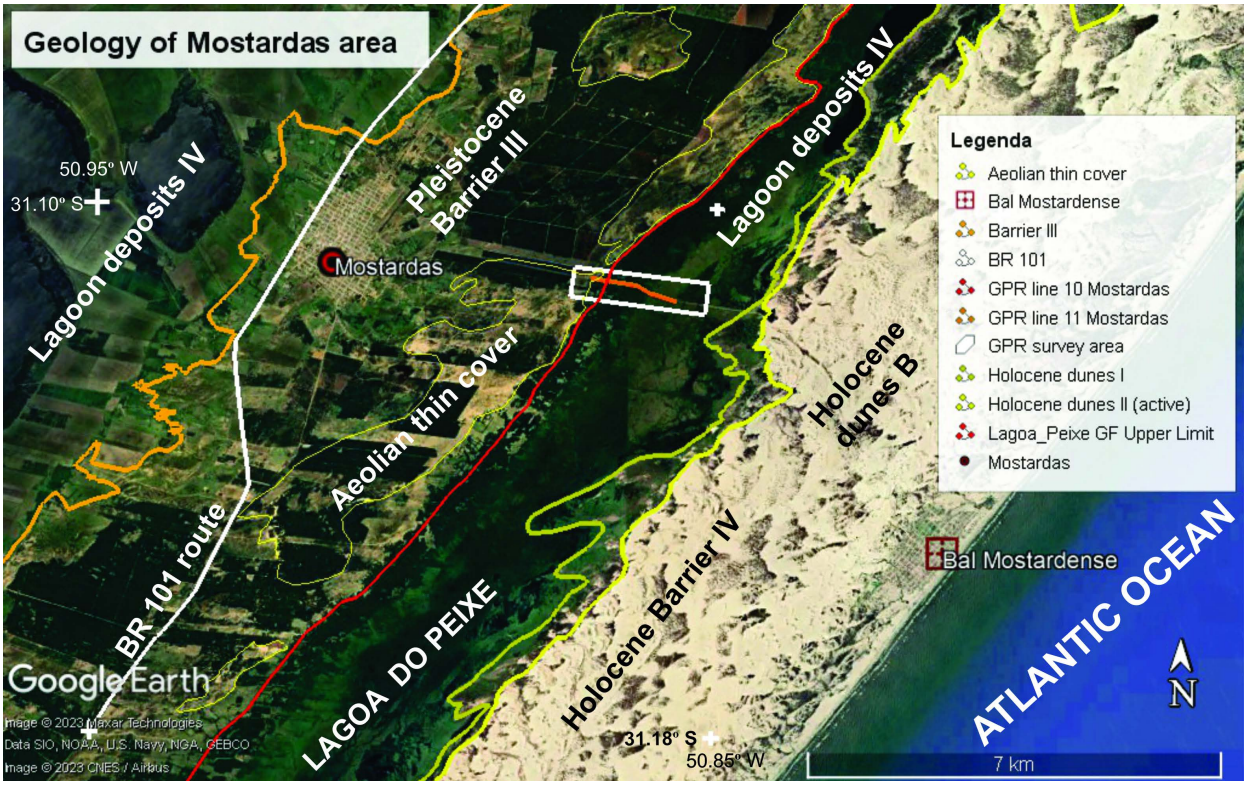

Figure 3. Geological map of the Mostardas area, with the location of the GPR survey lines. The extend of the GPR lines is shown in **Figure 11**.

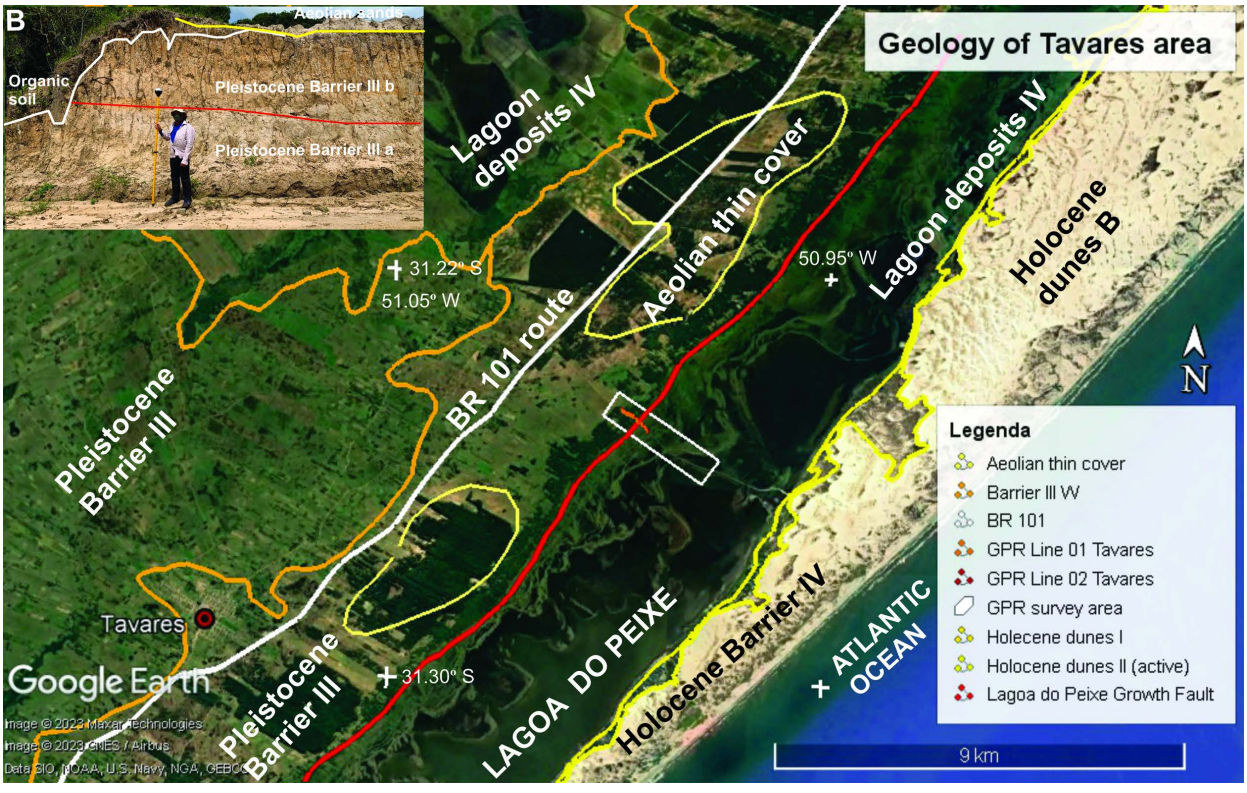

Figure 4. Geological map of the Tavares area, with the location of the GPR survey (A). Pleistocene Barrier III (B) crops out in the intersection of the fault trace and GPR lines (Talhamar Road). The extend of the GPR lines is shown in **Figure 9**.

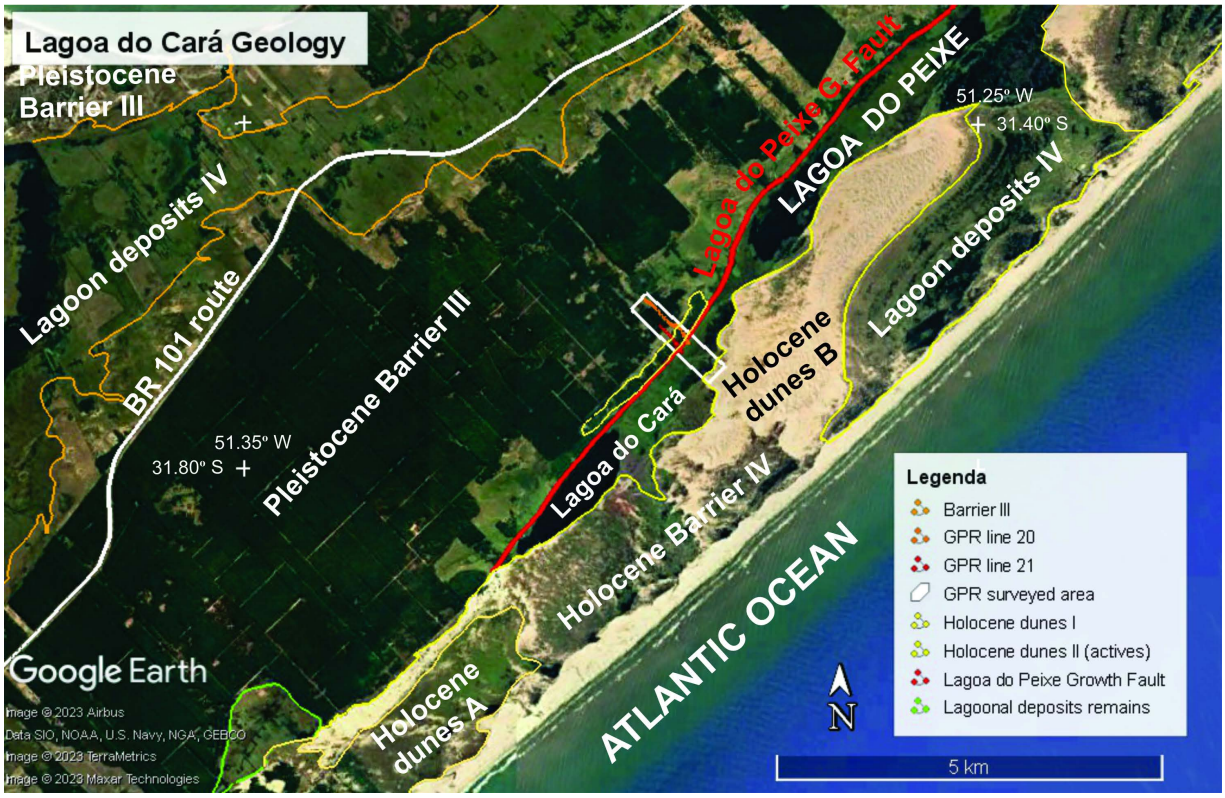

Figure 5. Geological map of the Lagoa do Cará area, with the location of the GPR survey lines. The extend of the GPR lines is shown in Figure 10.

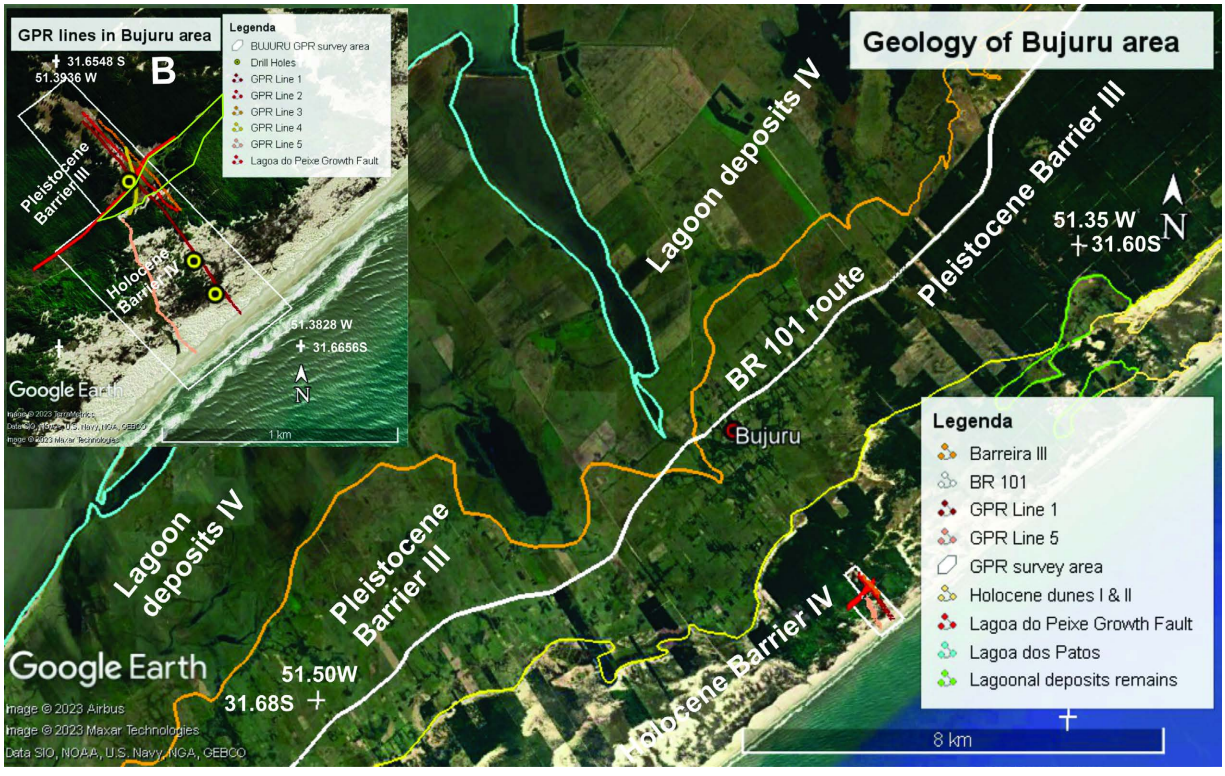

Figure 6. Geological map of the Bujuru area (A), with the location of the GPR survey lines and the drill holes along GPR line 1 (B). The extend of the GPR lines is shown in Figure 7.

The west fault-bounded margin of the Lagoa do Peixe, on the other hand, presents a number of wedge aprons that can be recognized to clog the lagoon. It is to be noted that these wedge aprons are in high angle to fault trace (see **Figure 4**) and do reflect erosion of the Pleistocene Barrier III footwall making up the scarp.

In the Bujuru area (**Figure 6**), the Holocene Barrier IV system almost completely covers the Holocene Lagoonal deposits and the Lagoa do Peixe Growth Fault; just a small window could be recognized, where GPR lines were surveyed. Two GPR lines were extended to the shoreface, since the upper peat layer does not crop out there, but 2 - 3 km to the southwest and to the northeast. In this way, the aim of the drilling campaign was to verify the peat layer continuity (drillholes 1 and 2, **Figure 7**), and it absence to the west of the fault (drillhole 3, **Figure 7**), were TDS (Transgressive Dune Sheets [11]) sediments lay directly over Pleistocene ones (Barrier III). Drillhole 3 also shows that no lagoonal deposit (such that underlaying peat in drillholes 2 and 1) is present over the Pleistocene sediments.

It is to be noticed, however, that 50 MHz GPR survey is not proper for distinguishing between different sediments and small-scale structures as seen in the drillholes. Then, drillhole features were correlated with higher-scale sedimentary structure and radarfacies given the enough EM properties contrast for the applied antenna.

Figure 7 shows the peat layer presence at depth in the Bujuru investigated area (**Figure 6(B)**), as predicted from its gentle folding structure. **Figure 7(A)** also shows that upper peat layer covers a well-defined radarfacies, which displays parallel, continuous reflections with wavelength larger than adjacent ones. This radarfacies is made up by more conductive material (clays, silt and organic matter—peat, for example) and is laid discordantly over previous radarfacies (see toplap feature in position below Borehole 1 in **Figure 7(A)**). Then, it is envisaged that peat layer cropping out at beach is a stratum covering the lower lagoonal radarfacies developed due to Lagoa do Peixe Fault.

A thin aeolian sand blanket (≤1 m thick) is widespread in the structural high made up by Pleistocene Barrier III (Borehole 3, **Figure 7**). But, it is locally thicker (up to 2 - 3 m) close to the fault scarp, where isolated or a sequence of few dunes can be recognized. They are better described as Transgressive Dune Sheets (TDS, [11]). Some of these thicker covers were emphasized in maps shown in **Figures 3-6**.

4. Geophysical Surveys: Fault Geometry and Kinematic

The radarfacies discrimination followed Neal [12] proposal. However, it was necessary to include fault truncation geometries for radarfacies boundary reflectors (**Figure 8**). Then, radarfacies discrimination was based on the following criteria: i) geometry of reflectors at boundaries, ii) shape of reflections, iii) dip of reflections, iv) relationship between reflections, v) reflections continuity, and vi) truncation of reflections.

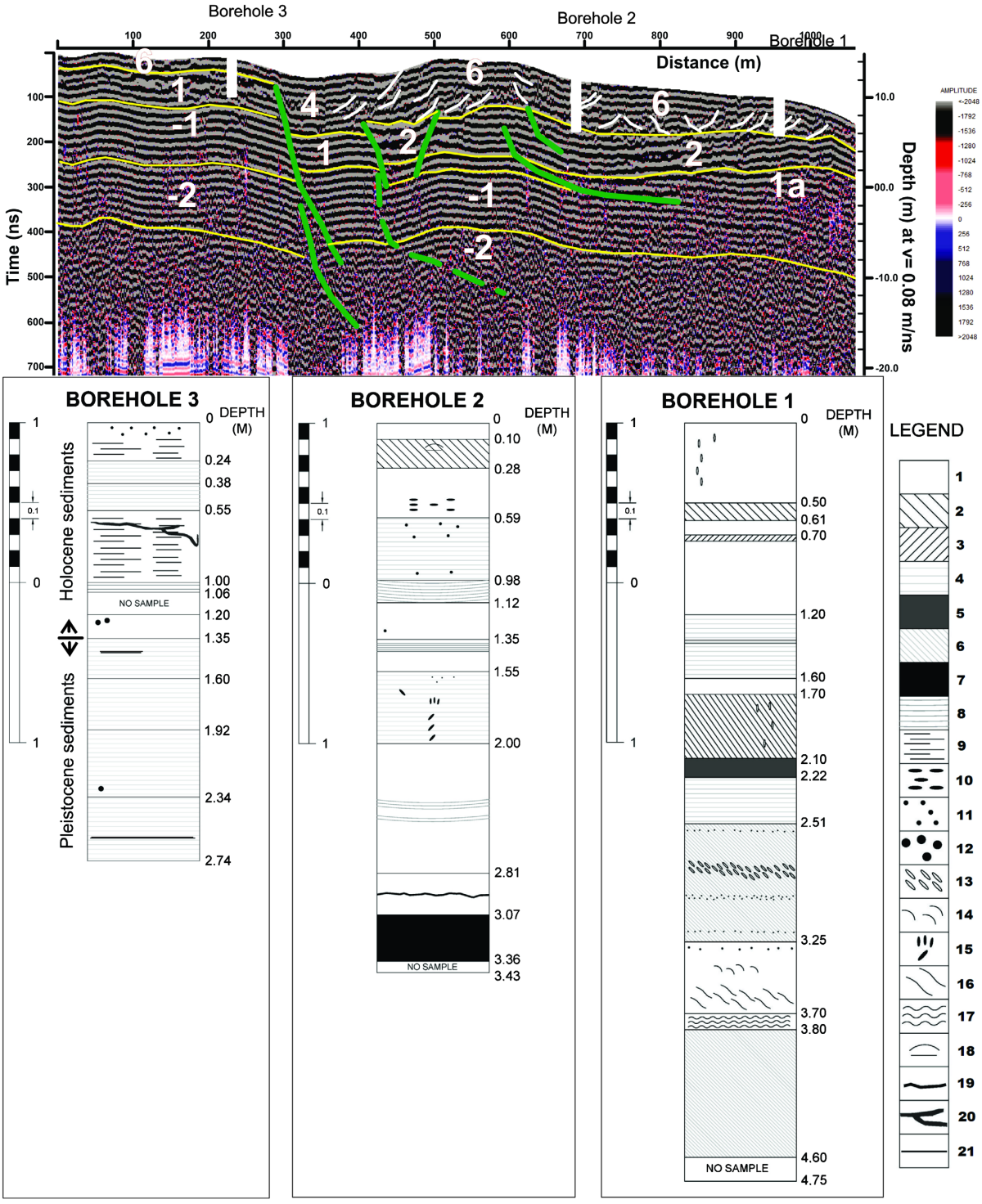

Figure 7. Radargram for Bujuru Line 01 (A) and boreholes description (B). Legend: 1) Light yellow sand; 2) Light yellow sand with coarse lamination (1 - 5 mm thick); 3) light yellow sand with gently inclined lamination (1 - 2 mm thick) and disseminated heavy minerals; 4) light yellow sand with thin horizontal lamination (1 mm) and disseminated heavy minerals; 5) Massive, dark gray sand with high quantity of heavy minerals; 6) Massive light yellow sand and disseminated heavy minerals; 7) Peat; 8) light yellow sand with gently arched lamination (1 mm); 9) isolated thin horizontal laminas of heavy minerals; 10) up to 2 cm recent root fragments; 11) small recent root fragments; 12) small disseminated shell fragments; 13) up to 1 cm shell fragments; 14) oxidized material; 15) oxidized (orange) dark gray sand; 16) heavy minerals concentration; 17) light yellow sand with fragmentary structure; 18) dispersed organic matter; 19) relicts of organic matter; 20) localized breccia structure; 21) dark yellow sand lamination.

4.1. Radarfacies and Surfaces Description

The description of the identified radar surface boundaries (s) and radarfacies (f) follows the chronologic sequence proposed by Neal and Roberts [17] and Neal [12]. **Table 2** summarizes the radar surface boundaries and radarfacies distinguished in the Lagoa do Peixe—Bujuru area.

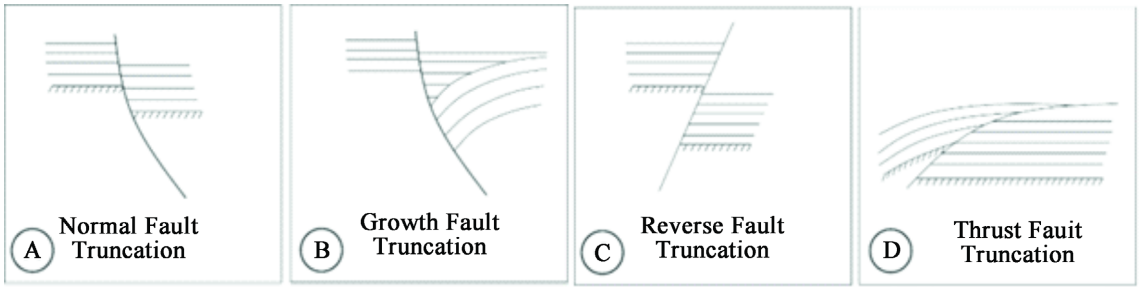

Figure 8. Fault truncation geometries for radar surface boundaries. (A) Normal fault truncation. (B) Growth fault truncation. (C) Reverse fault truncation. (D) Thrust fault truncation. These types of truncations can be observed in radargrams of [13] [14] [15] and [16].

Table 2. Summary of radar surface boundaries (**s**) and radarfacies (**f**) distinguished for GPR survey lines in the Lagoa do Peixe and their interpretation (Mostardas—Tavares—Lagoa do Cará—Bujuru, RS, Brazil).

Stage	Facies ID	DESCRIPTON	INTERPETATION
1	**LP-f_{n+1}-ps**	Pleistocene sediments (poorly compacted) cropping out west of Lagoa do Peixe escarpment (Barrier III).	Pleistocene sediments cropping out at the footwall top west of fault escarpment (Barrier III).
1a	**LP-f_{n+1}-pf**	Radarfacies underlying the lower lagoonal unit, displays regular reflections which are truncated (*toplap-offlap*) by its upper boundary.	Pre-fault radarfacies undergone hangingwall collapse and erosion.
	LP-s_{n+1}-gf	Upward concave listric geometry surface that truncate Pleistocene sediments (west) and lower lagoonal unit (east).	Listric gravitational growth fault. See also associated branching normal faults.
	LP-s_{n+2}-et	*Offlap-toplap* for reflectors underlying lower lagoonal unit; maybe an erosional truncation.	An erosional surface developed on the down-throwing hangingwall before fault controlled lagoonal accumulation.
2	**LP-f_{n+2}-pe**	Convex upward arcuted lower lagoonal unit, displaying *onlap* for lowermost reflections in the thickest zones, close to listric surface, and parallel reflections for uppermost strata.	Lagoonal accumulation during the first stage of fault displacement resulted in its convex geometry and greater thickness close to fault surface.
	LP-s_{n+3}-ol	Surface at the top of the lower lagoonal unit, in the outcropping peat layer, showing *onlap* reflections for overlying radarfacies.	An increase in water depth giving rise to *onlap* of horizontal sedimentary layer on both sides in the lagoon depocenter.
3	**LP-f_{n+3}-lag**	Horizontal reflections in a hangingwall triangular area close to listric surface, showing *onlap* upon lower lagoonal unit and listric surface.	Localized sediment accumulation while fault displacement advanced, during a second stage of fault displacement, clogging Lagoa do Peixe depocenter (triangular wedge).
	LP-s_{n+4}-dl	Discrete *onlap-downlap* features upon previous radarfacies on both margins of the Lagoa do Peixe.	Surface defining the vanishing stage of fault displacement, and the third stage of sediment accumulation in the Lagoa do Peixe.

Continued

4	**LP-f_{n+4}-lag**	Upward arcuated reflections at both Lagoa do Peixe margins, showing alternating *onlap-downlap* and *toplap-offlap* features.	Third stage of lagoonal sediment accumulation, characterized by the interbedding of lagoon sediments and sands from emersed areas on both sides of the Lagoa do Peixe.
5	**LP-f_{n+5}-es**	Dipping sinuous reflections in the Lagoa do Peixe escarpment, showing discrete downlap with lagoon sediment reflections.	Erosional degradation of the fault escarpment and deposition as interbedded layer of sands and lagoon sediments.
	LP-s_{n+n}-df	Minor truncation of inner reflections of radarfacies.	Minor listric normal faults merging into master one, or diachronic synthetic and antithetic normal faults.
	LP-s_{n+5}-dl	Irregular surface underlying recent dune sediments.	Surface upon which recent dune sediments prograde.
6	**LP-f_{n+6}-dm**	Horizontal and steeply dipping sigmoidal reflections, as also as thin horizontal reflection near the topographic surface.	Recent dunes and thin wind cover overlying previous sedimentary radarfacies: 6a—steeply dipping reflections: lateral limbs of recent dunes; 6b—horizontal reflections: frontal dune strata, and thin wind covers.

Types of radarfacies (f)	**Types of boundary surfaces (s)**
ps = Pleistocene sediments	**gf** = growth fault
pf = pre-fault unit underlaying lower lagoonal	**et** = erosional truncation
pe = lower lagoonal, underlying peat layer	**ol** = onlap
lag = sediments clogging the lagoon	**dl** = downlap
es = erosional sediments close to escarpment	**df** = diachronic normal faults
dm = recent dunes and thin wind covers (Upper Holocene)	

The most important GPR lines (Figure 9) were surveyed in the Talhamar Road, perpendicular to the Lagoa do Peixe escarpment. They display the most complete surface boundaries and radarfacies chronologic sequence. Figure 8 reveals a concave boundary surface (**LP-s_{n+1}-gf**) that is steeply dipping in the west-side, and gently dipping toward east. It truncates two main radarfacies: Pleistocene sediments (**LP-f_{n+1}-ps**), and the lower lagoonal unit (**LP-f_{n+2}-pe**).

The geophysical signature of the lower lagoonal radarfacies (**LP-f_{n+2}-pe**) shows it is westward dipping and convexly arcuated. It is also noticed that it is thicker close to the concave truncation surface (**LP-s_{n+1}-gf**). The lowermost reflectors of the lower lagoonal unit also show *onlap* features in the thicker segment close to the concave truncation.

The radarfacies underlying the lower lagoonal unit displays erosional truncation in its upper boundary (*toplap*), which is evidenced close to the concave boundary surface (**LP-s_{n+1}-gf**).

A close view of this boundary truncation surface (Figure 9(B)) shows a triangular feature delimitated by the upper boundary surface of the lower lagoonal radarfacies and the fault truncation surface. The inner reflectors in this triangle

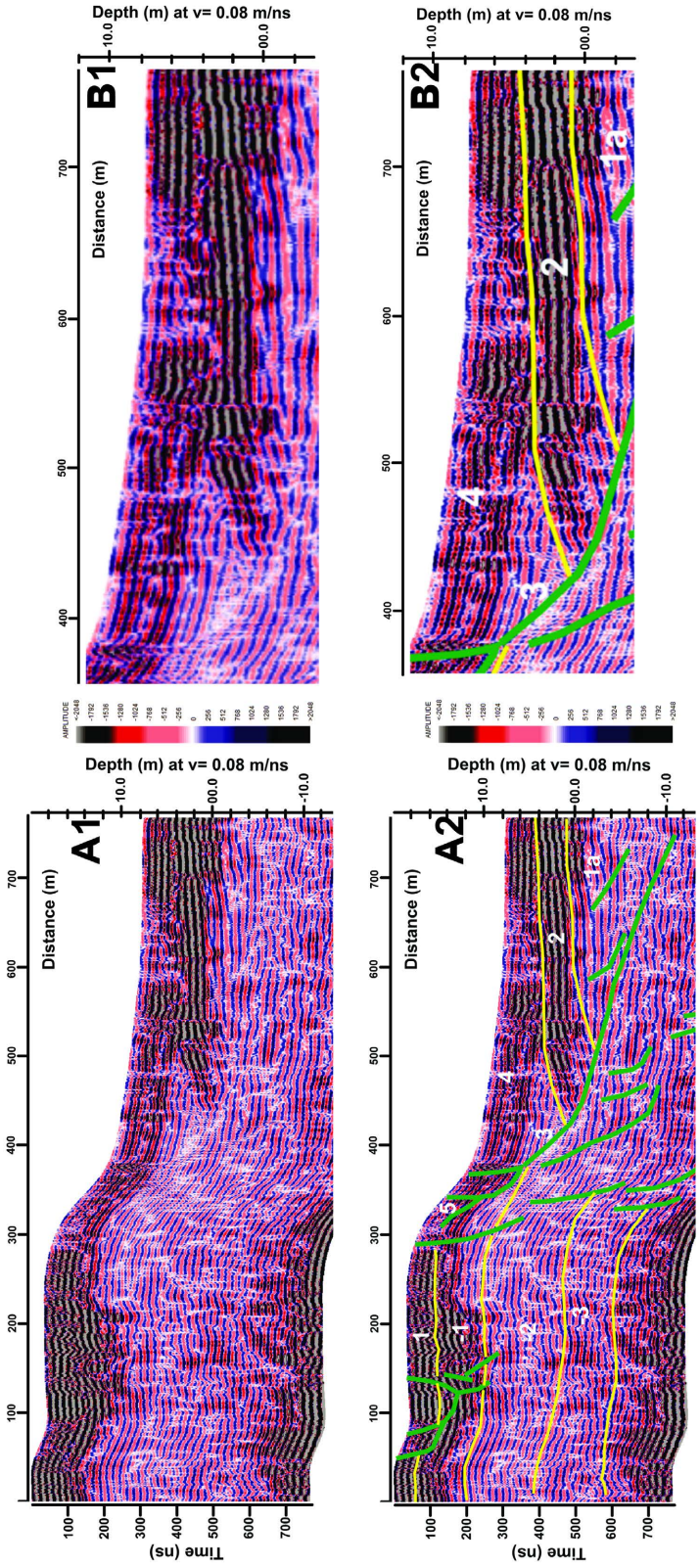

Figure 9. Radargram for Tavares area (Talhamar Road), that cut across fault escarpment in the Lagoa do Peixe National Park. Non-interpreted (1) and interpreted (2) radargrams are presented for evaluation. (A) Complete radargram, and (B) detail radargram showing the lower-thickened lagoonal, the triangular and the upper lagoonal radarfacies.

show onlap over both west and east boundary surfaces. The sedimentary unit overlying the lower lagoonal radarfacies in the fault hangingwall can be distinguished into two radarfacies: i) the triangular area radarfacies (**LP-f_{n+3}-lag**) restricted to the fault truncation hangingwall, which is onlapping both the concave truncation surface and the convex upper boundary for lower lagoonal radarfacies; and an ii) upper extended radarfacies (**LP-f_{n+4}-lag**), which display alternating *toplap-offlap* and *downlap-onlap* reflections features in both west and east sides of the lagoon.

The alternation of reflection features seems to indicate interbedding of lagoon sediments and that derived from erosion in emersed margins. This feature is better seen in Figure 10, where a thick Holocene dune lies on the top of footwall escarpment (structural high), and its east lateral strata (**LP-f_{n+6}-dm-6a**) flows into the lagoon. Escarpment degradation by erosion (**LP-f_{n+5}-es**) is also responsible for interbedding with lagoon sediments (**LP-f_{n+4}-lag**) (see Figure 11).

A number of diachronic synthetic and antithetic normal faults (**LP-s_{n+n}-df**) can be seen in the radargrams (e.g. Figure 10(A) and Figure 11). They cut across different radarfacies. The deeper ones often merge into the master growth fault or seem to merge to a master concave fault that could not be traced continuously at this resolution scale. A group of conjugated faults are close to the actual surface and are related to topographic depression.

It is to be noted that downthrow displacement of the growth fault in the Bujuru and Mostardas areas is lesser than in Tavares area. Bujuru and Mostardas areas near the tip zone of the main Lagoa do Peixe Growth Fault, which is covered by actual dune system (Holocene Barrier IV). It is also to be observed that the lower lagoonal unit (**LP-f_{n+2}-pe**) was not recorded close to the Lagoa do Peixe fault escarpment in the Lagoa do Cará (Figure 10(A)) and Mostardas (Figure 11). This indicates that lower lagoonal unit (**LP-f_{n+2}-pe**) was not deposited in that areas due to the fact that lateral growth fault propagation reaches those areas after lower lagoonal unit ceased to be deposited, or there exists some fault branch midway to the beach controlling lower lagoonal deposition.

4.2. Boundary Surfaces and Radarfacies Interpretation

The concave boundary surface (**LP-s_{n+1}-gf**) shows a number of features that can be interpreted as an emersed listric growth fault due to Quaternary gravitational neotectonic event in the RGSCP (Pelotas Basin): i) upward concave geometry, that flattens seaward; ii) exposes Pleistocene sediments at top of the footwall escarpment; iii) controls lower lagoonal sediments accumulation at hangingwall as it deepens (convex geometry and thickness toward the fault); iv) controls depocenter for lagoonal sedimentation of overlying radarfacies (triangular geometry area). These features are in accordance to that summarized by Chapman [18].

The kinematics of the listric growth fault may be linked to the deposition of the sedimentary radarfacies (Table 2). The subaerial evolution of this listric gravitational growth fault can be related to the rift-related depositional systems described by Prosser [19], but 1 - 2 orders of magnitude smaller.

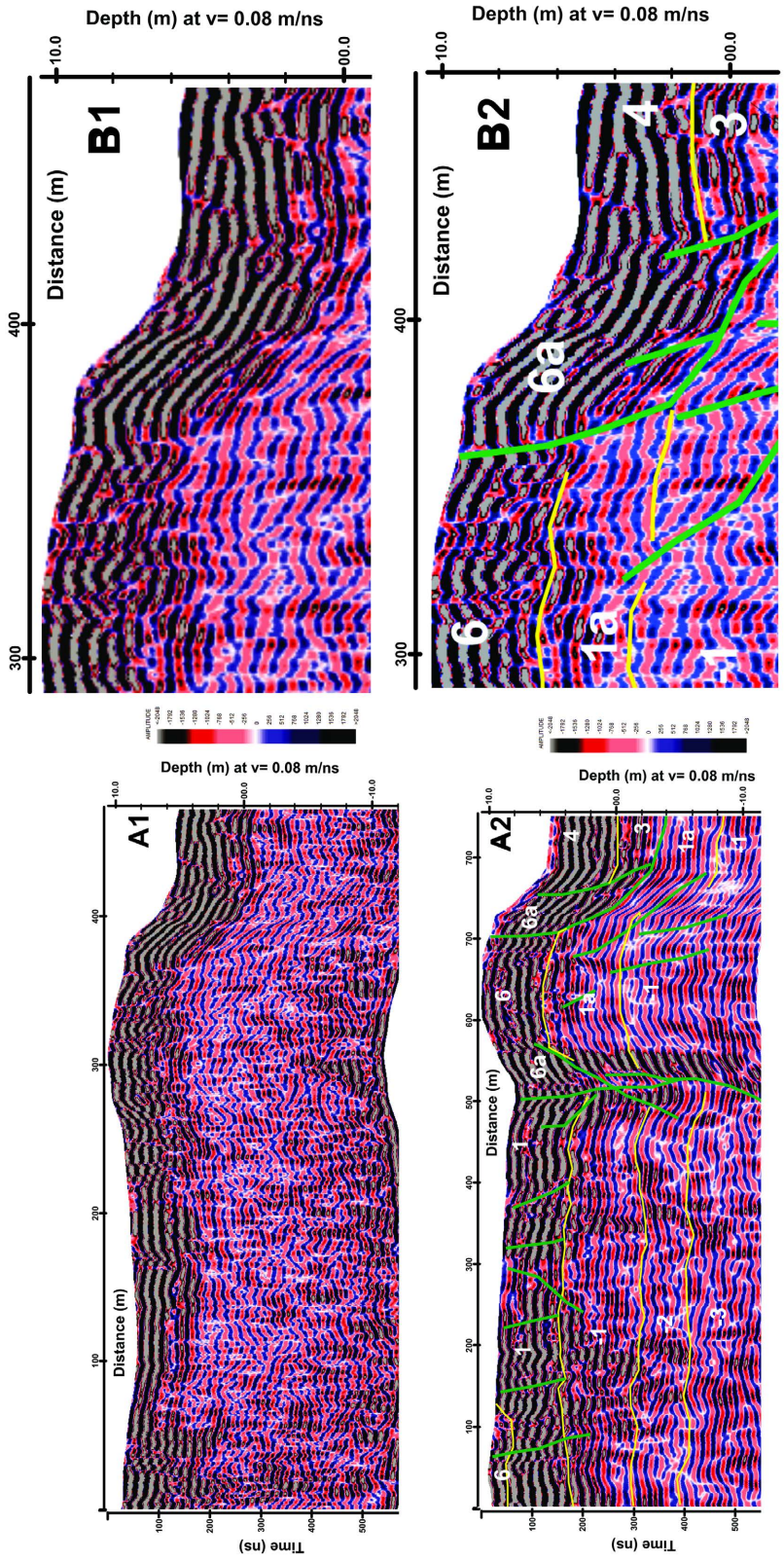

Figure 10. Radargram for Lagoa do Cará area (A), also cutting the fault escarpment. (B) A detail showing that reflections for lateral facies of the dune (6a) laying on the structural high are interbedded with lagoonal deposits (4). Non-interpreted (1) and interpreted (2) radargrams are presented for evaluation.

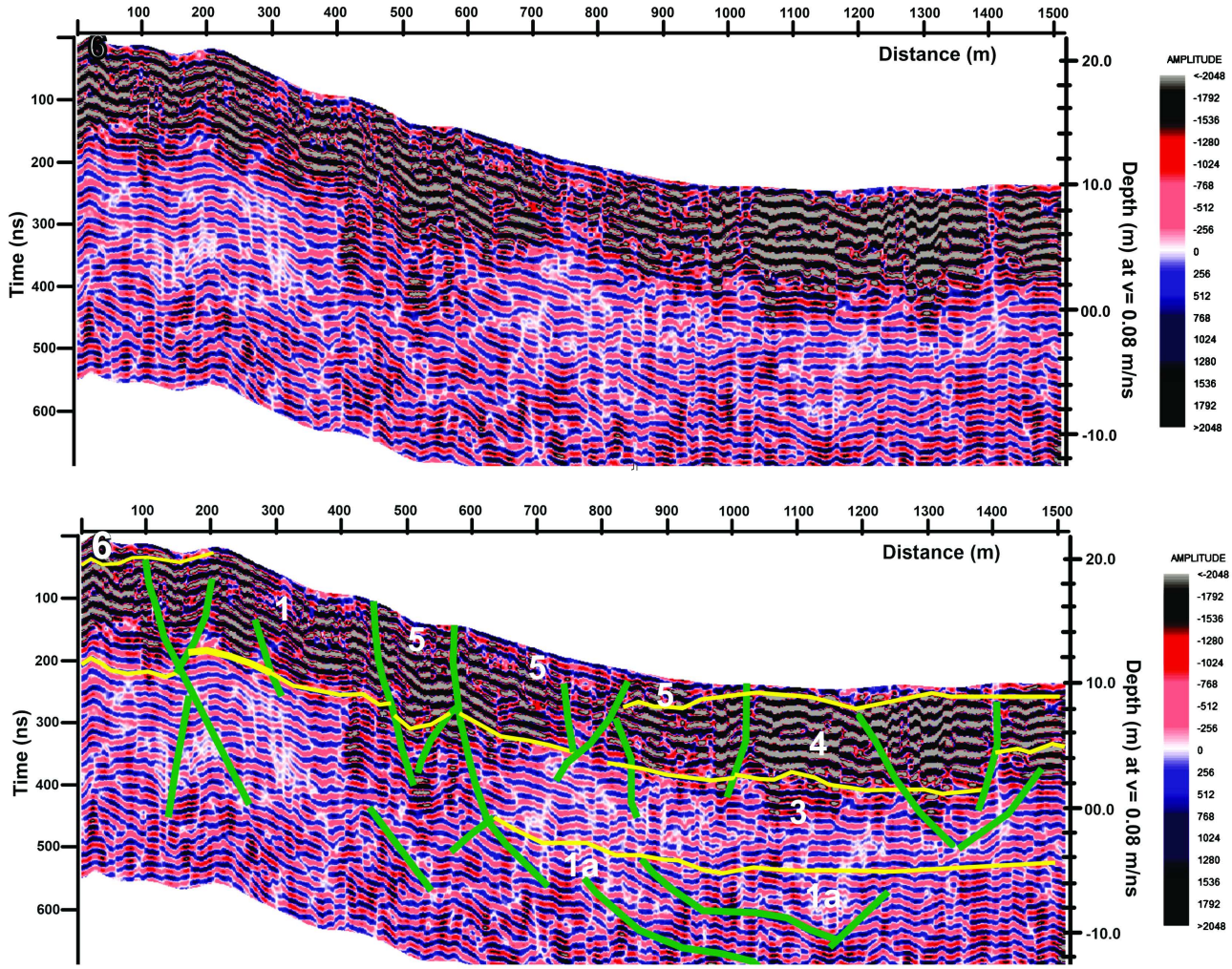

Figure 11. Radargram for Mostardas area, also cutting the fault escarpment. Non-interpreted (upper) and interpreted (lower) radargrams are presented for evaluation.

The evolution of sediment deposition while the listric gravitational fault displacement grows can also be distinguished into stages as proposed by Prosser [19]. The radarfacies underlying the lower lagoonal one is interpretated as a pre-fault sedimentary unit (**LP-f_{n+1}-pf**) since its upper boundary displays *of-flap-toplap* reflectors truncation.

The pre-fault sedimentary radarfacies (**LP-f_{n+1}-pf**) also shows a gentle convex arcuated geometry close to listric growth fault (**Figure 9**). Projection of this arc suggests that it dip less than the lower lagoonal radarfacies, and it seems that the pre-fault sedimentary strata underwent minor hangingwall collapse according to the fault displacement amount. In such a subaerial condition, the onset of the fault displacement can favour erosion by stream along strike in the faulted and rotating hangingwall.

The main stage of fault displacement is characterized by sedimentation in a broad area and the predominant accumulation of sediments higher in conductive properties, such as clays and peat, to give rise the lower lagoonal radarfacies

(**LP-f_{n+2}-pe**). The onlapping of the lowermost strata reflections close to the listric growth fault shows that fault displacement outpaces peat accumulation. Toward the top of lower lagoonal radarfacies, the sediment accumulation and fault displacement rates seem to keep pace.

The second stage of fault controlled lagoonal accumulation was taken in a restricted triangular area just in the Lagoa do Peixe depocenter (**LP-f_{n+3}-lag**), after a period of low sediment supply. The reflection geometry and *onlap* relationship suggest the fault displacement and sedimentation kept pace during this period. However, the gently eastward dipping upper reflections of this radarfacies suggest that sediment supply could have slightly surpassed fault displacement.

The vanishing stage of fault displacement is characterized by sedimentary supply from emersed areas on both margins of the Lagoa do Peixe (**LP-f_{n+4}-lag**). The alternate reflections (*onlap-downlap*, and *toplap-offlap*) at its margins suggests interbedding of lagoon sediments and sands. This is particularly distinguished in upper reflections close to the growth fault, due to escarpment erosion (**LP-f_{n+5}-es**), and sand flow of Holocene dune lateral limbs (**LP-f_{n+6}-dm**).

5. Discussion on Evolution of the Lagoa do Peixe Growth Fault and Sedimentation

The Lagoa do Peixe Growth Fault makes part of the gravitational tectonic affecting Pelotas Basin since Upper Miocene [20] and [21]. Santos [21] showed that Pelotas Basin gravitational tectonics started in the continental slope, and upper normal fault branches propagate westward into the platform.

The description and interpretation of radarfacies and surfaces (**Table 2**) show that it is possible to discuss an evolutionary model for this area of the RGSCP. But, for a complete preliminary scenario, it is interesting to introduce some absolute ages for key sedimentary units.

There exist few radiogenic ages for detailed peat layer investigation in the Lagoa do Peixe area. On the other hand, Bauermann [22] presented a detailed palynomorphic investigation, including ^{14}C ages for peat deposits cropping out north of Lagoa do Peixe. [22] investigated thick peat deposits and found 27.775 ± 155 - 12.948 ± 66 ^{14}C years BP to lowermost interval (Barrocadas area; 5.75 m and 3.10 m depth), 10.974 ± 49 ^{14}C years BP to middle interval (Águas Claras area; 2.70 m depth), and 3.879 ± 30 - 3.163 ± 29 ^{14}C years BP to the upper interval (Águas Claras—1.70 m depth—and Barrocadas—1.50 m depth—areas).

In the Bujuru area, Weschenfelder *et al.* [23] determined ages for two organic-rich mud intervals recovered in a drillcore: 9400 ± 140 Cal BP (23.2 m depth; ~10.000 ^{14}C years), and 7370 ± 150 Cal BP (5.0 m depth; ~8.300 ^{14}C years). In another core drilled in the same area, Medeanic *et al.* [24] found 7.370 ± 150 ^{14}C years BP (~6.330 ± 47 Cal BP) for organic-rich mud at 3.33 m depth.

Close to the SW end of the Lagoa do Cará, Dillenburg *et al.* [11] carried out a sequence of nine drillholes to recover material (2 shell samples, and 3 peat samples) for radiocarbon dating. Shell samples were collected close to the Atlantic

Ocean, in fine (muddy) sand underlying peat, and recorded ages of 3390 ± 130 and 3490 ± 70 ^{14}C years BP; it represents the upper stratum of the lower lagoonal radarfacies here described. Peat samples showed decreasing ages (1060 ± 70, 350 ± 60, and 380 ± 80 ^{14}C years BP) from east to west, where the Lagoa do Peixe escarpment anchors the peat and the underlying lagoonal sediments.

These results make possible to discusses an evolutionary model for the Lagoa do Peixe area. **Figure 12** shows the structural evolution of the Lagoa do Peixe Growth Fault and the sedimentation control in its tectonically sinking area.

The propagation of gravitational growth faults controls the local basin geometry and depocenter. The fault propagation rate controls mainly the sedimentary units' (radarfacies) geometry. The fault propagation, along its trend and dip, increases the area under tectonic subsidence, and then the local basin area for sedimentation. High fault propagation rates (outpacing sedimentation) develop an asymmetric basin and locate its depocenter close to fault. Low fault propagation displaces basin depocenter far away from fault and turns the basin geometry more symmetric. All these principles, derived from [19], apply to the Lagoa do Peixe Growth Fault and its local lagoonal basin (**Figures 12(A)-(D)**).

The first stage of fault displacement and sedimentation (Lower lagoonal radarfacies, **LP-f_{n+2}-pe**) seems to be initiated in the Lower Holocene (before 9400 ± 140 Cal BP, [24]) in this area. Several organic-rich mud layers are to be expected during the first stage of this rapidly subsiding, low sedimentation rate tectonic basin (**Figure 12(B)**).

In the second stage (**LP-f_{n+3}-lag**), the fault displacement and sedimentation keep pace, and sedimentation is restricted to the local basin depocenter. This radarfacies does not crop out and was not drilled yet for direct investigation (**Figure 12(C)**). The triangle edges of this radarfacies decreases in sizes toward the northeast and southwest fault tip lines, giving rise to a wedge-like sedimentary unit clogging the hangingwall of a fault-bounded local basin.

The third lagoonal stage (Upper lagoonal radarfacies, **LP-f_{n+4}-lag**) is characterized by an eastward basin depocenter dislocation, due to sedimentation rates largely outpacing fault displacement (**Figure 12(D)**). During this stage, the sedimentary influx comes from west (structural high = fault footwall) and east (local basin hinge zone). This upper lagoonal radarfacies also contains a number of peat layers, as recorded by Dillenburg *et al.* [11]: 1060 ± 70, 350 ± 60, and 380 ± 80 ^{14}C years BP. This observation is in accordance with this local basin geometry, as depicted in **Figure 12(D)**.

The peat layer cropping out in the beach (**Figure 7**) ages 1060 ± 70 ^{14}C years BP. It overlays the lower lagoonal radarfacies (**LP-f_{n+2}-pe**), which aged ~3500 ^{14}C years BP [11]. Then, there exists a ~2500 year's timespan between both radarfacies. This timespan can accomplish sedimentation of the second, wedge-like radarfacies.

Recent transgressive aeolian dunes migration (toward the southwest) is the main process of Lagoa do Peixe clogging. Erosion of the footwall structural high is also contributing to a minor scale. However, these processes were not detailed

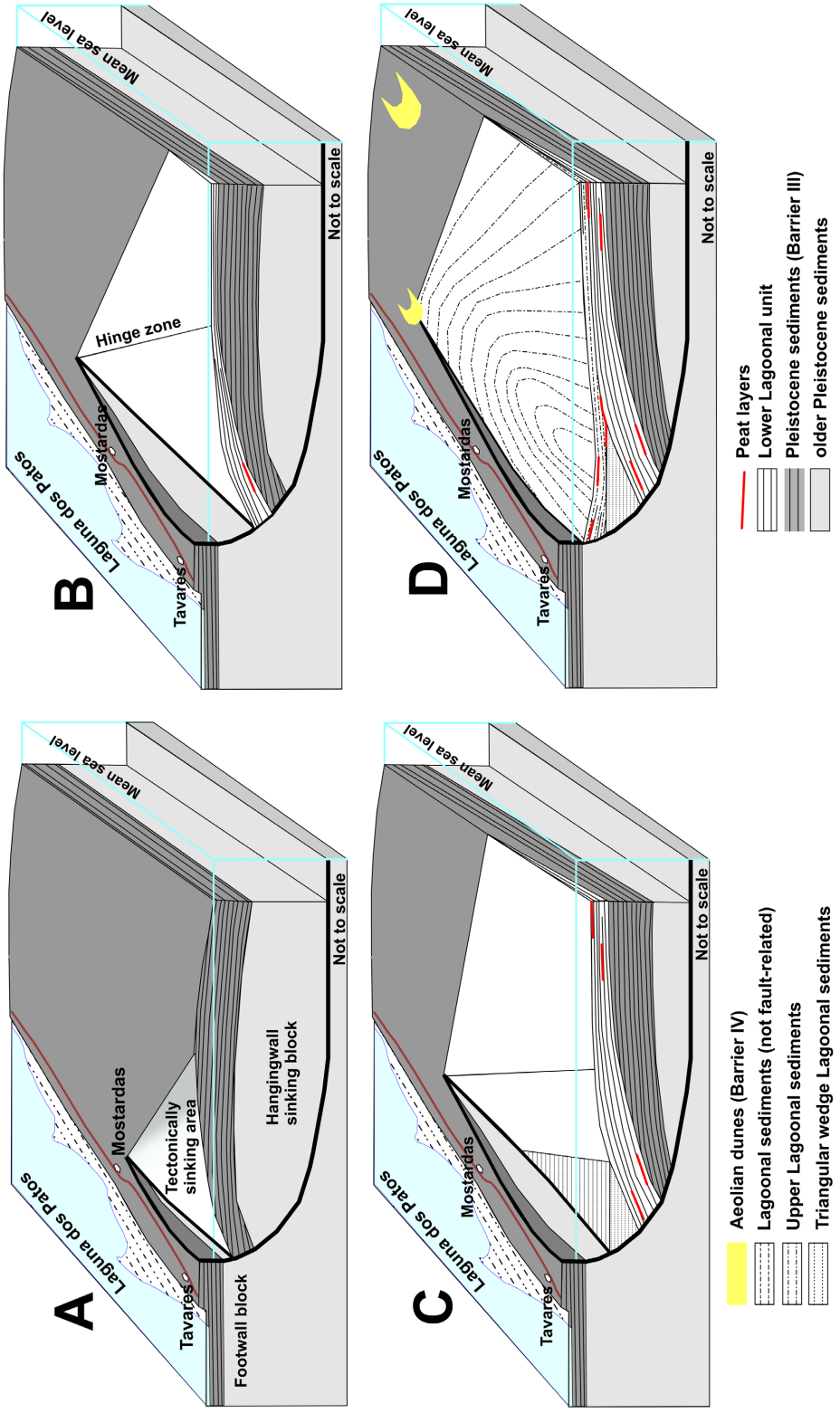

Figure 12. Evolutionary model for Lagoa do Peixe Growth Fault and linked sedimentation. (A) Growth fault initiation and propagation. (B) Propagation of fault tip zone (northeastward is shown) and deposition of the lower lagoonal radarfacies. (C) Additional fault propagation and sedimentation of the triangular wedge lagoonal radarfacies. (D) Last stages of fault propagation and sedimentation of the upper lagoonal radarfacies.

here since they are best evaluated with high frequency GPR investigations.

The presented and discussed geological features show that a thin-skinned gravitational sliding deformational episodes propagated to the RGS coastal plain. Da Fontoura [10] first reported thin-skinned gravitational sliding in the coastal plain of RGS. Thick and thin-skinned gravitational sliding in the Pelotas Basin were investigated in detail by Santos [21], but in its continental slope. The Lagoa do Peixe Growth Fault, then, proves that a large-scale gravitational tectonic was active in Pelotas Basin from the Upper Miocene to Holocene.

Thin-skinned gravitational sliding has long been reported and discussed in technical literature [25] [26], but for the platform slopes of Atlantic passive basins. These structural features are well known and studied in eastern Brazilian Atlantic margin [27] [28] where it is enabled by halokinesis, or in the northern basin [29]. However, the southernmost Brazilian basin does not have a salt layer, but is shale dominated. The sedimentary, stratigraphic, and tectonic implications for regional (platform) and local (coastal plain) are still under investigation. Then, it is soon to make an in-depth evaluation of the geological and geomorphic its consequence in Pelotas Basin and its coastal plain.

6. Conclusions

These geological and GPR surveys show that Lagoa do Peixe is a fault-controlled lagoon. The Lagoa do Peixe Growth Fault is a gravitational listric fault established in the Rio Grande do Sul Coastal Plain (RGSCP). The fault displacement controlled different stages of sedimentation in the tectonically subsiding Lagoa do Peixe, and it is nowadays under a clogging process due to erosion of fault escarpment, and Holocene aeolian dunes migration (Barrier IV).

The Lagoa do Peixe Growth Fault shows that, at least in this area, the non-tectonic lagoon-barrier systems approach should be reviewed. Growth fault, gravitationally driven control on geometry and sedimentation in the RGSCP introduces new complexities to the lagoon-barrier approach. Structural highs, fault overlapping zones, transfer faults are all significant underlying features, as well as fault displacement and sedimentation rates.

This new investigation approach is being carried on other areas, in order to evaluate the extent the gravitational tectonic took in the RGS coastal plain. It is clear, however, that it is part of a gravitational sliding process taking place from Upper Miocene in the Pelotas Basin platform slope to Holocene in the RGS coastal plain. Despite the length and significance of the Lagoa do Peixe Growth Fault, it is close to Atlantic Ocean, while other ones may be located landward, and are being investigated using the same approach here discussed.

Acknowledgements

Authors thank to Profa. Angélica Cirolini (UFSM), Prof. Alexandre F. Bruch (UFPel) and Prof. Christian Garcia Serpa (FURG) for DGPS support during geophysical surveys. B.S.F. also thanks to CNPq (Conselho Nacional de

Desenvolvimento Científico e Tecnológico) for Doctoral grant.

Conflicts of Interest

The authors declare no conflicts of interest regarding the publication of this paper.

References

[1] Villwock, J.A., Tomazelli, L.J., Loss, E.L., Dehnhardt, E.A., Horn Filho, N.O., Bachi, F.A. and Dehnhardt, B.A. (1986) Geology of the Rio Grande do Sul Coastal Province. In: Rabassa, J., Ed., *Quaternary of South America and Antarctic Peninsula*, CRC Press, London, 79-97. https://doi.org/10.1201/9781003079316-5

[2] Rosa, M.L.C.C., Barboza, E.G., Abreu, V.S., Tomazelli, L.J. and Dillenburg, S.R. (2017) High-Frequency Sequences in the Quaternary of Pelotas Basin (Coastal Plain): A Record of Degradational Stacking as a Function of Longer-Term Base-Level Fall. *Brazilian Journal of Geology*, **47**, 183-207. https://doi.org/10.1590/2317-4889201720160138

[3] Tomazelli, L.J. and Villwock, J.A. (1996) Quaternary Geological Evolution of Rio Grande do Sul Coastal Plain, Southern Brazil. *Anais da Academia Brasileira Ciências*, **68**, 373-382.

[4] Tomazelli, L.J., Dillenburg, S.R. and Villwock, J.A. (2000) Late Quaternary Geological History of Rio Grande do Sul Coastal Plain, Southern Brazil. *Revista Brasileira de Geociências*, **30**, 470-472. https://doi.org/10.25249/0375-7536.2000303474476

[5] Villwock, J.A. (1972) Contribuição à Geologia do Holoceno da Província Costeira do Rio Grande do Sul. Master's Thesis, Universidade Federal do Rio Grande do Sul, Porto Alegre.

[6] Fonseca, V.P. (2006) Estudos morfotectônicos aplicados à planície costeira do Rio Grande do Sul e adjacências. Ph.D. Thesis, Universidade Federal do Rio Grande do Sul, Porto Alegre.

[7] Strieder, A.J., Fontoura, B.S., Behling, J.S., Wetzel, R.S., Duarte, R.S.S., Silva, T.C., Mendes, P.R., Nobrega, A.A.V., Niencheski, L.F.H. and Calliari, L.J. (2015) Gravitational Tectonics Evidences at RGS (Brazil) Coastal Plain Using Ground Penetrating Radar. 2015 8*th International Workshop on Advanced Ground Penetrating Radar* (*IWAGPR*), Florence, 7-10 July 2015, 1-4. https://doi.org/10.1109/IWAGPR.2015.7292667

[8] Cooper, J.A.G., Green, A.N., Meireles, R.P., Klein, A.H.F., Souza, J. and Toldo, E.E. (2016) Sandy Barrier Overstepping and Preservation Linked to Rapid Sea Level Rise and Geological Setting. *Marine Geology*, **382**, 80-91. https://doi.org/10.1016/j.margeo.2016.10.003

[9] Cooper, J.A.G., Meireles, R.P., Green, A.N., Klein, A.H.F. and Toldo, E.E. (2018) Late Quaternary Stratigraphic Evolution of the Inner Continental Shelf in Response to Sea-Level Change, Santa Catarina, Brazil. *Marine Geology*, **397**, 1-14. https://doi.org/10.1016/j.margeo.2017.11.011

[10] Da Fontoura, B.S., Strieder, A.J., Corrêa, I.C.S., Mendes, P.R., Bruch, A.F. and Cirolini, A. (2024) Gravity Fault Subsidence and Beach Ridges Progradation in Quinta-Cassino (RS) Coastal Plain, Brazil. *Open Journal of Geology*, **14**, 177-195. https://doi.org/10.4236/ojg.2024.142011

[11] Dillenburg, S.R., Tomazelli, L.J. and Barboza, E.G. (2004) Barrier Evolution and

Placer Formation at Bujuru Southern Brazil. *Marine Geology*, **203**, 43-56. https://doi.org/10.1016/S0025-3227(03)00330-X

[12] Neal, A. (2004) Ground-Penetrating Radar and Its Use in Sedimentology: Principles, Problems and Progress. *Earth-Science Reviews*, **66**, 261-330. https://doi.org/10.1016/j.earscirev.2004.01.004

[13] Reiss, S., Reicherter, K.R. and Reuther, C.D. (2003) Visualization and Characterization of Active Normal Faults and Associated Sediments by High Resolution GPR. In: Bristow, C.S. and Joe, H.M., Eds., *Ground Penetrating Radar in Sediments*, Vol. 211, Geological Society, London, 247-255. https://doi.org/10.1144/GSL.SP.2001.211.01.20

[14] Christie, M., Tsoflias, G.P., Stockli, D.F. and Black, R. (2009) Assessing Fault Displacement and Off-Fault Deformation in an Extensional Tectonic Setting Using 3-D Ground-Penetrating Radar Imaging. *Journal of Applied Geophysics*, **68**, 9-16, https://doi.org/10.1016/j.jappgeo.2008.10.013

[15] Nobes, D.C., Jol, H.M. and Duffy, B. (2016) Geophysical Imaging of Disrupted Coastal Dune Stratigraphy and Possible Mechanisms, Haast, South Westland, New Zealand. *New Zealand Journal of Geology and Geophysics*, **59**, 426-435. https://doi.org/10.1080/00288306.2016.1168455

[16] Zhang, C., Wang, H., Liao, Y., Lu, Z. and Tang, J. (2016) Differential Control of Syndepositional Faults on Sequence Stratigraphy and Depositional Systems during Main Rift I Stage in the Southeastern Fault Zone of Qingxi Sag, Jiuquan Basin, Northwestern China. *Journal of Petroleum Exploration and Production Technology*, **6**, 145-157. https://doi.org/10.1007/s13202-015-0190-x

[17] Neal, A. and Roberts, C.L. (2001) Internal Structure of a Trough Blowout, Determined from Migrated Ground-Penetrating Radar Profiles. *Sedimentology*, **48**, 791-810. https://doi.org/10.1046/j.1365-3091.2001.00382.x

[18] Chapman, R.E. (1983) Early Deformation of Sedimentary Basins Growth Structures. In: Chapmann, R.E., Ed., *Developments in Petroleum Science Series*, Vol. 16, Elsevier, Amsterdam, 23-40. https://doi.org/10.1016/s0376-7361(08)70086-4

[19] Prosser, S. (1993) Rift-Related Linked Depositional Systems and Their Seismic Expression. In: Williams, G.D. and Dobb, A., Eds., *Tectonics and Seismic Sequence Stratigraphy*, Vol. 71, Geological Society, London, 35-66. https://doi.org/10.1144/GSL.SP.1993.071.01.03

[20] Castillo, L.L.A., Kazmierczak, T.S. and Chemale Junior, F. (2009) Rio Grande Cone Tectono-Stratigraphic Model-Brazil: Seismic Sequences. *Earth Sciences Research Journal*, **13**, 42-53.

[21] Santos, A.C.O. (2020) Tectônica Gravitacional no Cone do Rio Grande, Bacia de Pelotas (RS). Ph.D. Thesis, Universidade Federal do Rio Grande, Rio Grande.

[22] Bauermann, S.G. (2003) Análises palinológicas e evolução paleovegetacional e paleoambiental das turfeiras de Barrocadas e Águas Claras, Planície Costeira do Rio Grande do Sul, Brasil. Ph.D. Thesis, Universidade Federal do Rio Grande do Sul, Porto Alegre.

[23] Weschenfelder, J., Medeanic, S., Corrêa, I.C.S. and Aliotta, S. (2008) Holocene Paleoinlet of the Bojuru Region, Lagoa dos Patos, Southern Brazil. *Journal of Coastal Research*, **24**, 99-109. https://doi.org/10.2112/04-0369.1

[24] Medeanic, S., Dillenburg, S.R. and Toldo Junior, E.E. (2001) Novos dados palinológicos da transgressão marinha pós-glacial emsedimentos da Laguna dos Patos. *Revista Universidade Guarulhos*, *Geociências*, **6**, 64-76.

[25] Lundin, E.R. (1992) Thin-Skinned Extensional Tectonics on a Salt Detachment,

Northern Kwanza Basin, Angola. *Marine and Petroleum Geology*, **9**, 405-411. https://doi.org/10.1016/0264-8172(92)90051-F

[26] Brun, J.-P. and Fort, X. (2011) Salt Tectonics at Passive Margins: Geology versus Models. *Marine and Petroleum Geology*, **28**, 1123-1145. https://doi.org/10.1016/j.marpetgeo.2011.03.004

[27] Fernandez, B.M., Mohriak, W.U. and Menezes, P.T.L. (2003) Structural and Stratigraphic Aspects of Salt Tectonics in the Eastern Brazilian Margin: Evolution Model and Seismic Section Restoration. 8*th International Congress of the Brazilian Geophysical Society*, Rio de Janeiro, 14-18 September 2003, 6 p.

[28] Garcia, S.F.M., Letouzey, J., Rudkiewicz, J.-L., Danderfer Filho, A. and Lamotte, D.F. (2012) Structural Modeling Based on Sequential Restoration of Gravitational Salt Deformation in the Santos Basin (Brazil). *Marine and Petroleum Geology*, **35**, 337-353. https://doi.org/10.1016/j.marpetgeo.2012.02.009

[29] Souza, J.M.G., Cubas, N., Rabe, C., Letouzey, J., Divies, R., Praeg, D.B., Granjeon, D., Cruz, A.M., Guizan Silva, C.G., Reis, A.T. and Gorini, C. (2020) Controls on Overpressure Evolution during the Gravitational Collapse of the Amazon Deep-Sea Fan. *Marine and Petroleum Geology*, **121**, Article 104576. https://doi.org/10.1016/j.marpetgeo.2020.104576